DOI: 10.1002/ejic.201001104

A New Triazine-Based Tricompartmental Ligand for Stepwise Assembly of Mononuclear, Dinuclear, and 1D-Polymeric Heptacoordinate Manganese(II)/Azido Complexes

Animesh Das,[a] Serhiy Demeshko,[a] Sebastian Dechert,[a] and Franc Meyer*[a]

Keywords: Manganese / Azides / N ligands / Magnetic properties / Coordination polymer

A new ligand 2,4,6-tris[{*N*-methyl-*N*′-(pyridine-2-yl)methylidene}hydrazino]-1,3,5-triazine (L) has been synthesized from cyanuric chloride in two steps. The threefold symmetric L features three potentially tridentate {N_3} binding compartments. However, with Mn^{II} it binds a single metal ion using one of the triazine N atoms and two chelate arms. This {N_5} set forms the equatorial plane of a distorted pentagonal-bipyramidal metal ion environment, with a variety of ligands in axial positions. Five such Mn^{II} complexes have been isolated and characterized by X-ray crystallography. Complex **1** features axial water and nitrato-O ligands. In **5**, the latter is replaced by dicyanamide. Two terminal azido ligands are found in **3**. Depending on the ratio of L:Mn^{II}:azide, L may also adopt a bridging mode to give the dimeric species [{(H_2O)Mn^{II}L}(μ-1,3-N_3){LMn^{II}(NO_3)}](NO_3)$_2$ (**2**) or a 1D coordination polymer [(LMn^{II})(μ-1,3-N_3)]$_n$(NO_3)$_n$ (**4**). The basic {LMn^{II}} entity undergoes little structural variation in the series of complexes, which can be viewed as structural snapshots for the assembly of a Mn^{II}/azido polymeric chain from well-defined mononuclear building units. Magnetic coupling along the μ-1,3-azido linkage in the dimeric and 1D-extended complexes is weakly antiferromagnetic; the strength of the coupling is rationalized on the basis of the Mn–N–N angles and the dihedral angle τ along the azide ligand.

Introduction

The synthesis and characterization of new low-dimensional materials (one- or two-dimensional) that may show long-range cooperative magnetic phenomena has become a major focus of interest in the molecular magnetism arena in recent years.[1] Many groups are addressing the synthesis and study of discrete oligometallic molecules in an attempt to advance our understanding of the mechanism involved in magnetic coupling[2] and the targeted production of extended assemblies of paramagnetic metal ions with desirable magnetic properties.[3]

Azide (N_3^-) is among the heavily used bridging ligands in this field, since it can mediate strong magnetic coupling and can display great versatility in its coordination.[4] It is well established that azido bridges may link two or more metals ions in μ-1,3 (end-to-end, EE), μ-1,1 (end-on, EO), or even higher nuclearity binding modes.[5] Magnetic exchange mediated via an azido bridge can be ferro- or antiferromagnetic, depending on the bridging mode and bonding parameters. It has been widely stated that exchange is generally ferromagnetic in nature for the EO mode and antiferromagnetic for the EE mode,[4–6] although an increasing number of exceptions have been reported.[7] The structures and magnetic properties of metal azido systems are obviously sensitive to the coligands employed. To date, numerous coligands have been introduced into metal–azido systems, giving rise to an abundant range of polymeric complexes that show a wide variety of magnetic properties.[4–6,8–11] Among the first-row transition metal azides, high-spin Mn^{II} is of particular interest as a spin carrier because it contains the highest possible number of unpaired electrons for a d metal ion.[8,12]

1,3,5-Triazine derivatives are receiving increased attention as ligand scaffolds for several reasons: (i) starting from cheap cyanuric chloride various triazine derivatives are readily available;[13] (ii) the *meta* positioning of the N donors in the ring may give rise to ferromagnetic coupling by the spin-polarisation mechanism;[14] (iii) the threefold symmetry of the 1,3,5-triazine core is an attractive feature in the field of supramolecular chemistry and crystal engineering.[15] However, the electron-deficient triazine has proven quite reluctant towards binding several metal ions by the ring N atoms, which has stimulated the development of more sophisticated triazine-based scaffolds with three donor substituents providing suitable chelate compartments.[16]

Here we report about the new tricompartmental ligand 2,4,6-tris[{*N*-methyl-*N*′-(pyridine-2-yl)methylidene}hydrazino]-1,3,5-triazine (L) and we explore the behavior of this particular scaffold in Mn/azide chemistry. Ligand L has been found to bind one metal ion instead of the anticipated three, and an interesting series of heptacoordinate Mn^{II} complexes has been developed, which provides structural

[a] Institut für Anorganische Chemie, Georg-August-Universität, Tammannstrasse 4, 37077 Göttingen, Germany
Fax: +49-551-39-3063
E-mail: franc.meyer@chemie.uni-goettingen.de

snapshots of the stepwise assembly of 1D-polymeric Mn^{II}/azido chains through mono- and dinuclear species. In this paper we describe the synthesis, characterisation, and magnetic properties of these complexes.

Results and Discussion

Synthesis and General Characterisation

The new ligand was synthesized by condensation of 2-pyrdinecarboxaldehyde with 2,4,6-tris(*N*-methylhydrazino)-1,3,5-triazine[17] in methanol (Scheme 1). L was isolated as a white powder in 94% yield and characterised by NMR and IR spectroscopy as well as elemental analysis.

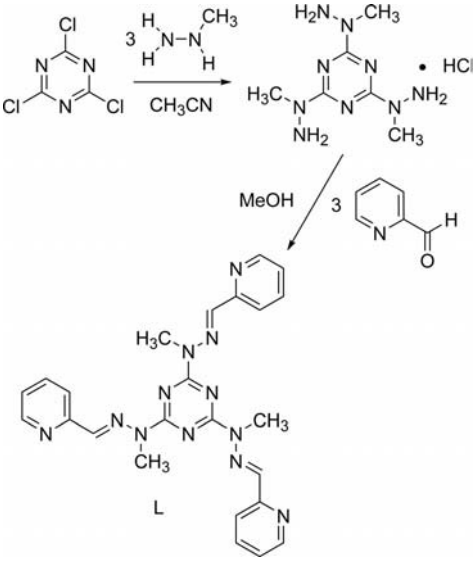

Scheme 1. Synthesis of L.

Ligand L features a central triazine ring with three dangling arms and three potentially tridentate pockets. The result of the reaction of L with $Mn(NO_3)_2{\cdot}xH_2O$ and NaN_3 is strongly dependent on the ratio of the reactants, but in all cases only a single Mn^{II} ion was directly bound to the triazine N atom and further embraced by two of the chelate substituents, even if three or more equivalents of $Mn(NO_3)_2{\cdot}xH_2O$ were used with respect to L. Careful control of the reaction conditions resulted in the isolation and full characterization of a series of complexes ranging from the Mn^{II} complex of L without any azide (**1**), which can be viewed as a precursor to the mononuclear complex with terminal azido ligands (**3**), continuing to an azido-linked dimeric species (**2**) and finally to the azido-bridged 1D polymeric chain system (**4**; Scheme 2).

Crystals of $[Mn(L)(NO_3)(H_2O)](NO_3)$ (**1**) were obtained by mixing L and $Mn(NO_3)_2{\cdot}xH_2O$ in methanol, followed by slow evaporation of the solvent. The 1D polymeric complex **4** was isolated when L, the metal salt, and sodium azide were combined in equimolar amounts (1:1:1) in methanol at room temperature. Upon reflux under otherwise identical conditions, however, a mixture of the **4** and the mononuclear compound **3** was formed. Complex **3** can also

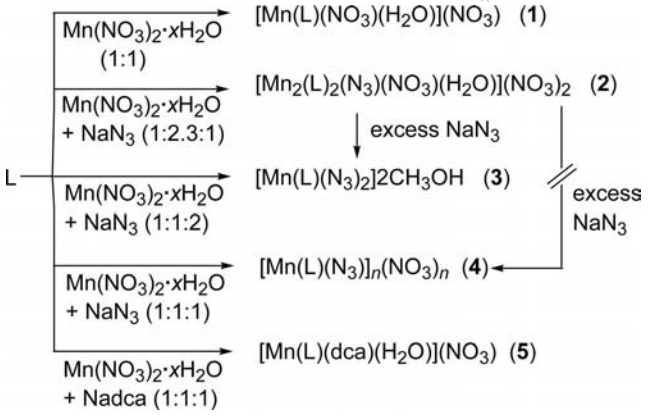

Scheme 2. Synthetic scheme of complexes **1**–**5**.

be prepared directly when the reactants are used in 1:1:2 ratio, or by treating **2** with an excess of NaN_3. Somewhat surprisingly, complex **2** is best obtained from L, $Mn(NO_3)_2{\cdot}xH_2O$, and NaN_3 in the presence of an excess of the metal salt.

The molecular structure of complex **1** is shown in Figure 1 (top). A single heptacoordinate manganese ion is found in a strongly distorted pentagonal-bipyramidal environment with five N donor atoms in the basal plane: two pyridine N atoms, two sp^2 hydrazone N atoms from two chelate strands, and the N1 atom of the central triazine ring. A similar pincer-like binding motif has recently been reported for cobalt(II) and lead(II) complexes of a triazine-based ligand with only two hydrazone arms.[18,19] Steric repulsion between the pyridyl ends of the substituents (2.31 Å between the H atoms in the pyridyl-6 positions) enforces a twisted conformation of the pincer array. Thus the dihedral angle between the two planes N1–N5–N6–Mn1 and N1–N8–N9–Mn1 is 13.16°. The axial positions in **1** are filled by an oxygen atom of a water molecule and a nitrato O atom. Heptacoordination is not unusual for triazine-based Mn^{II} compounds and has previously been observed in some complexes with tris(2-pyridyl)triazine.[20]

The axial ligands in **1** are easily varied with retention of the pincer-like motif, as shown by the isolation of **5** from the reaction of L, $Mn(NO_3)_2{\cdot}xH_2O$, and sodium dicyanamide. The molecular structure of **5** (Figure 1, middle) is essentially identical that of **1** except the axial nitrate is replaced by a N-bound dicyanamide. The helical twist of the basal coordination strand is similar to that in **1** (7.9° between the two planes N1–N5–N6–Mn1 and N1–N8–N9–Mn1). A feature to note is the *cisoid* conformation of the N11 and N12 atoms in **5**, which is unusual as repulsion between the N lone pairs should give rise to a *transoid* orientation, as in 2,2′-bipyridine.[21] It seems that there is hydrogen bonding between N12 to the water molecule of an adjacent complex molecule [d(O1···N12) = 2.774(2) Å] in the solid-state structure of **5**; however, we do not discuss hydrogen bonding interactions in detail because the SQUEEZE routine was used in the crystallographic analysis of **5** to remove disordered parts. In **3** (Figure 1, bottom) both axial positions are occupied by EO bound azido li-

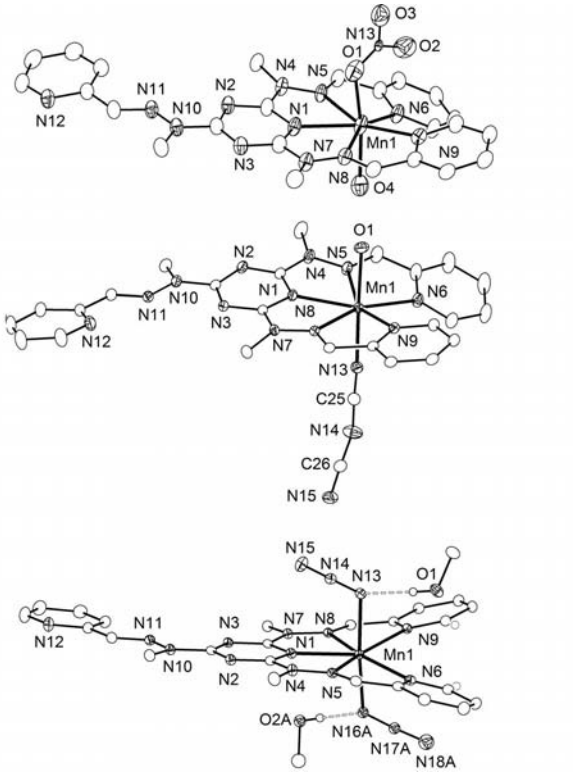

Figure 1. ORTEP plots (30% probability thermal ellipsoids) of the molecular structures of of **1** (top), **5** (middle), and **3** (bottom). Most hydrogen atoms and counterions are omitted for clarity. Selected bond lengths [Å] and angles [°] for **1**: Mn1–O1 2.158(4), Mn1–O4 2.162(4), Mn1–N1 2.273(3), Mn1–N6 2.337(3), Mn1–N5 2.353(3), Mn1–N9 2.355(3), Mn1–N8 2.370(3); O1–Mn1–O4 166.16(16), O1–Mn1–N1 79.15(15), O4–Mn1–N1 92.05(14), O1–Mn1–N6 111.60(16), O4–Mn1–N6 82.21(14), N1–Mn1–N6 133.22(12), O1–Mn1–N5 86.77(14), O4–Mn1–N5 99.55(14), N1–Mn1–N5 66.32(11), N6–Mn1–N5 68.99(11), O1–Mn1–N9 85.46(13), O4–Mn1–N9 93.16(14), N1–Mn1–N9 133.64(11), N6–Mn1–N9 93.11(11), N5–Mn1–N9 156.16(12), O1–Mn1–N8 83.07(15), O4–Mn1–N8 83.59(13), N1–Mn1–N8 65.95(11), N6–Mn1–N8 156.41(12), N5–Mn1–N8 132.24(11), N9–Mn1–N8 68.95(11). Selected bond lengths [Å] and angles [°] for **5**: Mn1–N13 2.1840(17), Mn1–O1 2.1950(16), Mn1–N1 2.2760(14), Mn1–N9 2.3480(15), Mn1–N5 2.3508(16), Mn1–N8 2.3665(15), Mn1–N6 2.3921(16); N13–Mn1–O1 178.43(6), N13–Mn1–N1 94.10(6), O1–Mn1–N1 87.45(6), N13–Mn1–N9 93.98(6), O1–Mn1–N9 84.78(6), N1–Mn1–N9 133.38(5), N13–Mn1–N5 100.21(6), O1–Mn1–N5 80.60(7), N1–Mn1–N5 66.62(5), N9–Mn1–N5 154.71(6), N13–Mn1–N8 88.35(5), O1–Mn1–N8 92.10(7), N1–Mn1–N8 65.56(5), N9–Mn1–N8 68.88(5), N5–Mn1–N8 131.86(5), N13–Mn1–N6 83.90(6), O1–Mn1–N6 95.18(7), N1–Mn1–N6 133.46(6), N9–Mn1–N6 93.06(6), N5–Mn1–N6 68.04(6), N8–Mn1–N6 159.83(5). Selected bond lengths [Å] and angles [°] for **3**: Mn1–N16B 2.178(15), Mn1–N16A 2.186(2), Mn1–N13 2.2138(16), Mn1–N1 2.2854(16), Mn1–N5 2.3731(14), Mn1–N9 2.3734(14), Mn1–N8 2.3837(15), Mn1–N6 2.4161(16), O1···N13 2.834(2), O2A···N16A 2.835(3), O2B···N16B 2.61(2); N16B–Mn1–N13 175.5(4), N16A–Mn1–N13 173.48(7), N16B–Mn1–N1 86.9(4), N16A–Mn1–N1 95.01(7), N13–Mn1–N1 89.40(6), N16B–Mn1–N5 96.6(4), N16A–Mn1–N5 101.88(7), N13–Mn1–N5 84.28(5), N1–Mn1–N5 66.18(5), N16B–Mn1–N9 96.3(5), N16A–Mn1–N9 89.15(6), N13–Mn1–N9 84.34(5), N1–Mn1–N9 133.15(5), N5–Mn1–N9 157.35(6), N16B–Mn1–N8 82.9(4), N16A–Mn1–N8 84.37(7), N13–Mn1–N8 93.14(6), N1–Mn1–N8 65.51(5), N5–Mn1–N8 131.64(5), N9–Mn1–N8 68.55(5), N16B–Mn1–N6 90.3(4), N16A–Mn1–N6 86.31(7), N13–Mn1–N6 94.14(6), N1–Mn1–N6 133.44(5), N5–Mn1–N6 68.03(5), N9–Mn1–N6 93.37(5), N8–Mn1–N6 159.71(5), O1–H1···N13 176(3), O2A–H2A···N16A 169.4, O2B–H2B···N16B 144.3.

gands. Here the helical twist characterized by the angle between the two planes N1–N5–N6–Mn1 and N1–N8–N9–Mn1 is 9.7°. Methanol solvent molecules are attached by hydrogen bonds to the two metal-bound N atoms of the axial azido ligands [*d*(O···N) = 2.6 to 2.8 Å].

The molecular structure of **2** is depicted in Figure 2. It features two pincer-type subunits similar to **1**, **3**, and **5**, which are linked by a μ-1,3 (EO) azide. A water molecule occupies the remaining axial position at Mn2, and a nitrate is *O*-bound to Mn1. This distinction causes some asymmetry in the bimetallic array, which is also reflected by the slightly different angles Mn1–N33–N34 and Mn2–N35–N34 (155.1° and 149.9°, respectively). The dihedral angle Mn1–N33–N35–Mn2 (τ) is 156.9°.

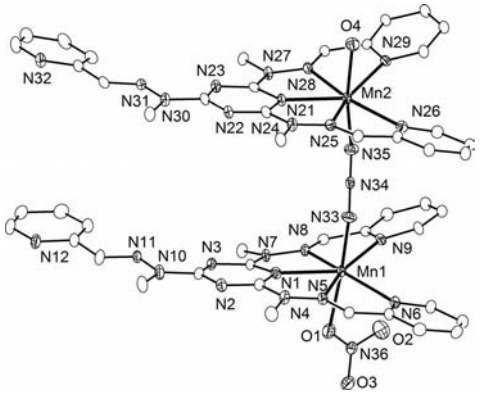

Figure 2. ORTEP plot (30% probability thermal ellipsoids) of the molecular structure of **2**. Hydrogen atoms and counterions are omitted for clarity. Selected bond lengths [Å] and angles [°] for **2**: Mn1–N33 2.216(5), Mn1–O1 2.226(5), Mn1–N1 2.269(4), Mn1–N9 2.324(5), Mn1–N5 2.356(5), Mn1–N6 2.360(4), Mn1–N8 2.377(4), Mn2–O4 2.189(4), Mn2–N35 2.199(5), Mn2–N21 2.284(4), Mn2–N26 2.366(4), Mn2–N29 2.372(5), Mn2–N28 2.376(5), Mn2–N25 2.392(5), Mn1···Mn2 6.560(1); N33–Mn1–O1 167.3(2), N33–Mn1–N1 93.73(18), O1–Mn1–N1 80.23(16), N33–Mn1–N9 84.14(19), O1–Mn1–N9 108.16(19), N1–Mn1–N9 132.81(16), N33–Mn1–N5 83.90(19), O1–Mn1–N5 83.47(19), N1–Mn1–N5 66.30(15), N9–Mn1–N5 158.14(15), N33–Mn1–N6 92.77(18), O1–Mn1–N6 83.69(16), N1–Mn1–N6 133.92(17), N9–Mn1–N6 93.23(16), N5–Mn1–N6 69.17(16), N33–Mn1–N8 103.63(17), O1–Mn1–N8 84.30(17), N1–Mn1–N8 66.54(16), N9–Mn1–N8 68.26(15), N5–Mn1–N8 132.60(15), N6–Mn1–N8 153.40(17), O4–Mn2–N35 169.71(18), O4–Mn2–N21 90.41(16), N35–Mn2–N21 99.11(18), O4–Mn2–N26 92.15(15), N35–Mn2–N26 84.21(17), N21–Mn2–N26 133.14(17), O4–Mn2–N29 80.37(16), N35–Mn2–N29 90.27(18), N21–Mn2–N29 132.41(16), N26–Mn2–N29 94.04(16), O4–Mn2–N28 93.37(16), N35–Mn2–N28 87.09(17), N21–Mn2–N28 65.53(16), N26–Mn2–N28 160.50(17), N29–Mn2–N28 68.53(15), O4–Mn2–N25 82.25(16), N35–Mn2–N25 105.12(18), N21–Mn2–N25 66.01(15), N26–Mn2–N25 68.03(16), N29–Mn2–N25 154.47(15), N28–Mn2–N25 131.29(15).

The polymeric chain of **4** determined by X-ray crystallography is depicted in Figure 3 (top), with details of the individual subunit shown at the bottom of Figure 3. Pincer-type building blocks {LMn^{2+}} are connected by μ-1,3 (EE) azido ligands to give the anticipated extended 1D structure. Structural parameters of the metal ions in **4** are very similar to those of the dinuclear complex **2**, except for the bond angles involving the azide coligands. The angles Mn1′–

N15–N14 and Mn1–N13–N14 are almost identical (around 159°), which implies a symmetric μ-1,3 azide binding mode. The dihedral angle Mn1–N13–N15–Mn1′ (τ) is 170.4°. This angle is a major factor that determines the magnetic coupling between the azide-bridged metal ions.[4]

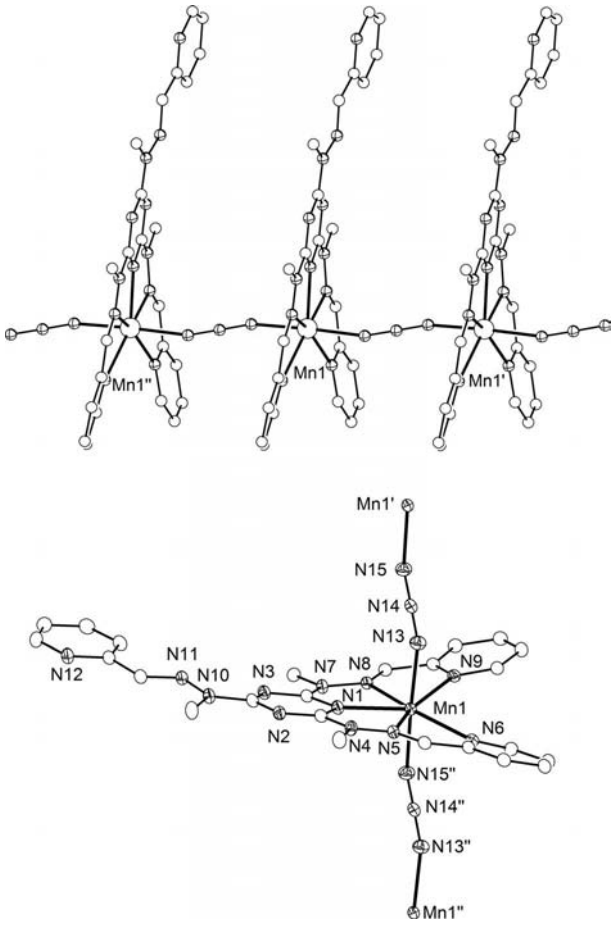

Figure 3. ORTEP plot (30% probability thermal ellipsoids) of the molecular structure of single subunit (bottom) and the chain structure of **4** (top). Hydrogen atoms, counterions, and solvent molecules are omitted for clarity. Selected bond lengths [Å] and angles [°] for **4**: Mn1–N15′′ 2.221(3), Mn1–N13 2.257(3), Mn1–N1 2.267(2), Mn1–N5 2.340(2), Mn1–N6 2.347(2), Mn1–N9 2.361(2), Mn1–N8 2.361(2), N15–Mn1′ 2.221(3), Mn1···Mn1′ 6.7116(4); N15′′–Mn1–N13 176.56(9), N15′′–Mn1–N1 93.59(9), N13–Mn1–N1 89.26(9), N15′′–Mn1–N5 99.93(9), N13–Mn1–N5 82.97(9), N1–Mn1–N5 66.39(7), N15′′–Mn1–N6 84.45(9), N13–Mn1–N6 94.93(9), N1–Mn1–N6 134.33(8), N5–Mn1–N6 69.06(7), N15′′–Mn1–N9 93.69(9), N13–Mn1–N9 82.96(8), N1–Mn1–N9 132.96(8), N5–Mn1–N9 155.75(8), N6–Mn1–N9 92.63(7), N15′′–Mn1–N8 84.31(8), N13–Mn1–N8 95.11(9), N1–Mn1–N8 65.99(7), N5–Mn1–N8 132.36(7), N6–Mn1–N8 157.41(8), N9–Mn1–N8 68.63(7). Symmetry transformations used to generate equivalent atoms: (′) 1 + *x*, *y*, *z*; (′′)–1 + *x*, *y*, *z*.

Comparison of all Mn–N or Mn–O distances in **1**–**5** reveals somewhat shorter bonds to the triazide moiety and the coordinating O or N atoms in axial positions compared to the Mn–N bonds involving the iminopyridine chelate arms (Table 1). The N/O_{ax}–Mn–N/O_{ax} angles are not far from 180°, with the strongest deviation in case of **1** and **2** (Table 2). All bond lengths and angles are comparable with those reported for the structurally related macrocyclic Mn^{II} complexes of 2,13-dimethyl-3,6,9,12,18-pentaazabicyclo-[12.3.1]octadeca-1(18),2,12,14,16-pentaene in which the metal atom is coordinated by seven donor atoms.[22]

Table 1. Selected bond lengths [Å] for **1**–**5**.

Atoms	**1**	**2**[a]	**3**[b]	**4**	**5**
Mn1–N1	2.273(3)	2.269(4) 2.284(4)	2.285(2)	2.267(2)	2.276(1)
Mn1–N5	2.353(3)	2.356(5) 2.392(5)	2.373(1)	2.340(2)	2.351(2)
Mn1–N6	2.337(3)	2.360(4) 2.366(4)	2.416(2)	2.347(2)	2.392(2)
Mn1–N8	2.370(3)	2.377(4) 2.376(5)	2.384(2)	2.361(2)	2.367(2)
Mn1–N9	2.355(3)	2.324(5) 2.372(5)	2.373(1)	2.361(2)	2.348(2)
Mn1–N/O_{ax}	2.158(4) 2.162(4)	2.216(5) 2.226(5) 2.189(4) 2.199(5)	2.18(2) 2.19(2) 2.214(2)	2.221(3) 2.257(3)	2.184(2) 2.195(2)
Mn···Mn	–	6.560(1)	–	6.712(4)	–

[a] Mn1–Nx and Mn2–N2x. [b] N16A/B.

Table 2. Selected bond angles [°] for **1**–**5**.

Atoms	**1**	**2**[a]	**3**[b]	**4**	**5**
N/O_{ax}–Mn–N/O_{ax}	166.2(2)	167.3(2) 169.7(2)	173.5(1) 175.5(4)	176.6(1)	178.4(1)

[a] Mn1–Nx and Mn2–N2x. [b] N16A/B.

Characterization of the series of complexes **1**→**3**→**2**→**4** is noteworthy because this provides the structural basis for all stages of the assembly of an azido-bridged 1D coordination polymer, starting from the Mn^{II} building block devoid of the bridging units (**1**), attachment of the azido ligands (**3**), dimer formation (**2**), and the final 1D chain system (**4**).

Infrared spectroscopy can be a useful tool to investigate details of azide coordination. In accordance with the very similar azido binding modes in **2**–**4**, band positions in the azide stretching region exhibit only minor variations in this series of complexes. Compounds **3** and **4** give strong absorptions at 2037 and 2054 cm^{-1}, respectively. However, complex **2** shows two intense bands at 2108 cm^{-1} and 2061 cm^{-1}; this may possibly reflect the somewhat asymmetric nature of the μ-1,3 azido linkage in **2**.

Magnetic Properties

Magnetic susceptibility data were collected for all the complexes in the temperature range from 295 to 2.0 K. No significant field dependence was observed when data were measured at applied fields of 0.2 and 0.5 T. The temperature dependence of the molar magnetic susceptibility χ_M and of the product $\chi_M T$ for all new complexes is shown in Fig-

ure 4. The observed $\chi_M T$ value at 295 K is 4.36 $cm^3 K mol^{-1}$ (corresponding to an effective moment μ_{eff} = 5.91 μ_B) for **1**, 4.26 $cm^3 K mol^{-1}$ (5.84 μ_B) for **3**, 4.40 $cm^3 K mol^{-1}$ (5.94 μ_B) per metal ion for **4**, and 4.35 $cm^3 K mol^{-1}$ (5.90 μ_B) for **5**.

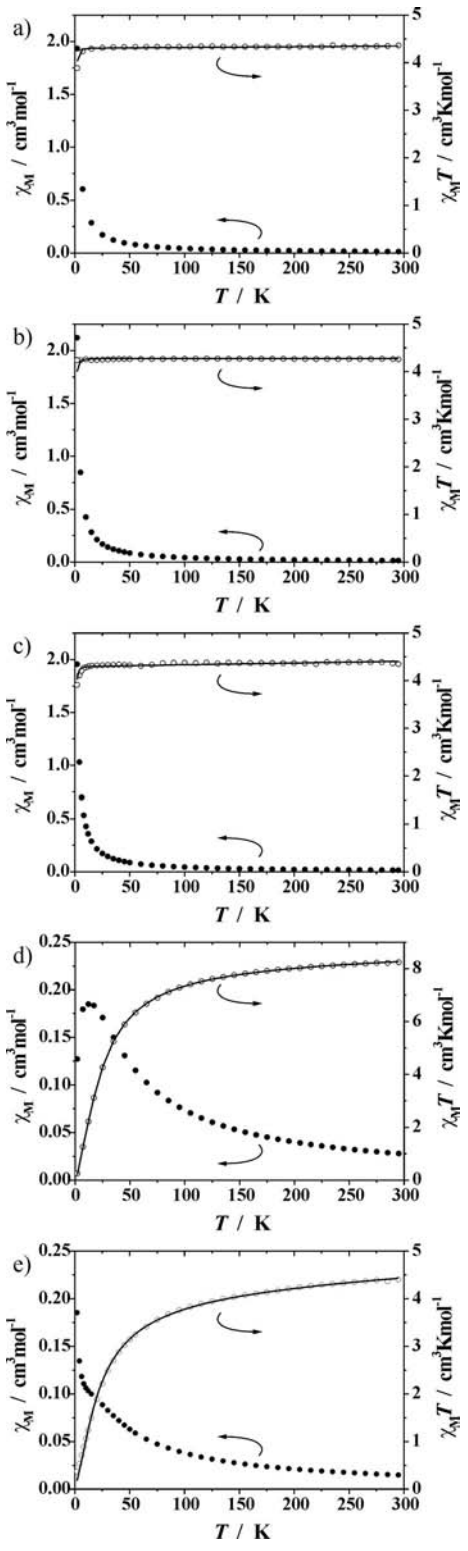

Figure 4. Plots of χ_M (solid circles) and $\chi_M T$ (open circles) vs. temperature for **1** (a), **3** (b), **5** (c), **2** (d), **4** (e), at 0.5 T. The solid black lines represent the simulated curves.

These values are close to the theoretical value expected for a single high-spin Mn^{II} ion with g = 2.0 (4.38 $cm^3 K mol^{-1}$ or μ_{eff} = 5.92 μ_B). For the binuclear complex **2**, the observed $\chi_M T$ value at 295 K is 8.24 $cm^3 K mol^{-1}$ (corresponding to an effective moment μ_{eff} = 8.12 μ_B), which is slightly smaller than the theoretical value expected for two uncoupled Mn^{II} ions (8.75 $cm^3 K mol^{-1}$ or μ_{eff} = 8.37 μ_B for g = 2.0). For the mononuclear compounds **1**, **3**, and **5**, the $\chi_M T$ value remains constant with decreasing the temperature and the data obey the Curie law, confirming that there are no significant intermolecular magnetic interactions between adjacent molecules. A slight decrease of $\chi_M T$ at very low temperatures may be due to saturation. For compounds **2** and **4** that feature μ-1,3 bridging azido ligands, $\chi_M T$ values gradually decrease upon lowering the temperature and finally tend towards zero (Figure 4, d and e). This is typical for overall antiferromagnetic coupling and an S = 0 ground state. Experimental data were simulated using a fitting procedure to the appropriate Heisenberg–Dirac van Vleck (HDvV) spin Hamiltonian according to Equation (1)[23] (for **2**) and (2)[24] (for **4**).

$$\hat{H} = -2J\hat{S}_1 \cdot \hat{S}_2 + g\mu_B(\hat{S}_1 + \hat{S}_2)B \quad (1)$$

$$\hat{H} = -2J \Sigma \hat{S}_i \cdot \hat{S}_{i+1} \quad (2)$$

Given the very similar metal ion environment in **1**–**5**, the g value for all complexes was uniformly fixed at 2.0 (which is reasonable for high-spin Mn^{II}). This required including a minor amount of diamagnetic impurity (*DI*) in the fitting procedure; temperature-independent paramagnetism (*TIP*) was also included. Table 3 summarizes the magnetic parameters obtained from best-fit analyses. The results confirm that there exists an intramolecular antiferromagnetic exchange interaction between the Mn^{II} ions in both **2** and **4**.

Table 3. Best fit parameters of magnetic data analysis for complexes 1–5.

	g	J [cm^{-1}]	*DI* [%][a]	*TIP* [10^{-6} $cm^3 mol^{-1}$][a]
1	2.0	–	1.6	150 (fixed)
2	2.0	–1.72	2.8	584
3	2.0	–	2.3	0
4	2.0	–1.02	0.6	1100
5	2.0	–	1.8	364

[a] *TIP* and *DI* were included according to $\chi_{calc} = (1 - DI)\cdot\chi + TIP$.

Magnetostructural correlations for single μ-1,3-azido-bridged Mn^{II} complexes have revealed that two geometric parameters, the Mn–N–N angles and the dihedral angle τ along the azide ligand, are of major importance.[25] Extended Hückel molecular orbital (EHMO) calculations showed that the antiferromagnetic coupling features a maximum for Mn–N–N angles close to 110°, but should become very small for Mn–N–N angles near 160°. Evaluation of the effect of the torsion angle τ affords similar qualitative results: the antiferromagnetic interaction should be maximized for a planar arrangement of the Mn^{II} ions and the azido bridge, but should be minimized for large torsion angles. The interesting conclusion derived from these calculations is that the μ-1,3-azido-bridged Mn^{II} com-

Table 4. Some structural and magnetic parameters for dinuclear and 1D Mn^{II} compounds with single EE azido bridges.

Compounds[a]	Mn–N–N (deg.)	τ (deg.)	J	Ref.
4	158.9/159.0	170.4	–1.02	this work
$[Mn_2(phen)_4(\mu_{1,3}\text{-}N_3)(N_3)_2]BPh_4 \cdot 0.5H_2O$	133.9/124.0	127.2	–1.15	[26]
2	155.1/149.9	156.9	–1.72	this work
$[Mn(\mu_{1,3}\text{-}N_3)(dpyo)Cl(H_2O)_2]\cdot nH_2O$	127.6/159.8	180	–1.75	[27]
$[Mn_2(L^1)_3(\mu_{1,3}\text{-}N_3)]_n(ClO_4)_{3n}$[b]	162.9	180	–1.8	[28]
$[Mn(H_2O)(\mu_{1,3}\text{-}N_3)(N_3)(quinaz)_2]_n$	142.6/137.3	180	–2.18	[29]
$[Mn(R/S\text{-}L)_2(\mu_{1,3}\text{-}N_3)]_n(ClO4)_n$	136.7/151.5	25.4	–2.35	[30]
$[Mn(L^2)(\mu_{1,3}\text{-}N_3)]_n(PF_6)_n$	125.2/118.8	143.3	–2.4	[22]
$[Mn_2(TLA)_2(\mu_{1,3}\text{-}N_3)(N_3)_2]\cdot(ClO_4)$	141.2	180	–2.99	[31]
$[Mn(L^3)(\mu_{1,3}\text{-}N_3)]_n(ClO_4)_n$	161.3/124.3	95.0	–3.3	[32]

[a] phen = 1,10-phenanthroline, dpyo = 4,4′-dipyridyl-*N*,*N*′-dioxide, L^1 = [*N*,*N*′-bis(pyridine-2-yl)]ethane-1,2-diamine, quinaz = quinazoline, *R*/*S*-L = *R*-pyridine-2-carbaldehyde-imine, L^2 = 2,13-dimethyl-3,6,9,12,18-pentaazaicyclo[12.3.1]octadeca-1(18),2,12,14,16-pentaene, TLA = tris(6-methyl-2-pyridyl methyl)amine, L^3 is the bidentate Schiff base obtained from the condensation of pyridine-2-carbaldehyde with 4-methoxyl aniline. [b] Dinuclear complex from magnetic point of view.

plexes, in contrast to Ni^{II} or Cu^{II} complexes, should always be antiferromagnetic, even if the torsion angles are close to 90° or if the Mn–N–N angles are near to 160°. The reason is that Mn^{II} complexes − apart from a main σ-interaction of the e_{2g}-orbitals of the metal ions with nonbonding π-MOs of the azido bridge − a pπ-dπ interaction pathway between the azido bridge and two of the t_{2g} orbitals (d_{xz}, d_{yz}) is active. While the σ-interaction strongly depends on the angle and becomes negligible for appropriate angles, the π-interaction is always different from zero and therefore the antiferromagnetic contribution to the overall coupling does never fully disappear. Thus the geometric variations of the central Mn^{II}–azide core can only attenuate the strength of the antiferromagnetic coupling but cannot change the sign of the interaction. The analysis of all known dinuclear and 1D Mn^{II} compounds with a single EE azido bridge confirms this finding (Table 4).

The Mn–N–N angles are slightly more obtuse in **4** (158.9/159.0°) than those in **2** (155.1/149.9°). Consequently the stronger coupling in **2** can be explained by a better overlap of the e_g^2 orbitals of the Mn^{II} ions with nonbonding π-MOs of the azido bridge through σ-interactions.

Conclusions

In this study, a new triazine-based ligand with threefold symmetry and three potentially tridentate $\{N_3\}$ binding pockets has been developed. In contrast to our original aim, however, L was found to not bind three but only one single Mn^{II} center, using one of the triazine N atoms and two of its chelate arms. Molecular models suggest that the methyl groups at the hydrazone N atoms may cause undesired steric interactions with a metal ion bound to the adjacent triazine N atom, thus disfavouring the involvement of the latter N atoms in metal coordination.

Using Mn^{II} and azide as a complementary ligand, however, an interesting series of complexes with heptacoordinate metal ions was isolated and fully characterized. This comprises the basic $\{LMn^{II}\}$ building block with labile water and nitrato O ligands (**1**), a related mononuclear complex with two azido ligands in axial positions (**3**), a dimer where two $\{LMn^{II}\}$ units are spanned by a μ-1,3-azide (**2**), and finally a 1D-polymeric Mn^{II}/azido chain system (**4**). Taken together these complexes provide structural snapshots for the assembly of a 1D coordination polymer from well defined mononuclear entities. As expected, the μ-1,3-azido linkages mediate antiferromagnetic coupling between the Mn^{II} ions, albeit this is relatively weak, as observed previously for Mn^{II} compounds with single EE azido bridges. Subtle differences in the strengths of the coupling can be related to the Mn–N–N angles and the dihedral angle τ along the azide ligand, which are the dominant parameters in Mn^{II}/azido magnetochemistry.

Experimental Section

Materials and Methods: Solvents were purified by established procedures.[33] All other chemicals were purchased from commercial sources and used as received. Microanalyses were performed by the Analytical Laboratory of the Institute for Inorganic Chemistry at Georg-August-University Göttingen using an Elementar Vario EL III. IR spectra were recorded using a Digilab Excalibur Series FTS 3000 spectrometer and UV/Vis spectra of solutions and solids (diffuse reflectance) with a Varian Cary 5000 spectrometer at room temperature. Mass spectra were measured using a Finnigan MAT 8200 (EI), a Finnigan MAT 95 (FAB-MS), or a Finnigan MAT LCQ mass spectrometer (ESI-MS). NMR spectra were recorded with a Bruker Avance 500 at room temperature (^{1}H 200.13 MHz, ^{13}C 50.3 MHz) and calibrated to the residual proton and carbon signals of the solvent ($CDCl_3$ δ_H = 7.26 ppm, δ_C = 77.0 ppm). Magnetic data were measured with a Quantum-Design MPMS-5S SQUID magnetometer equipped with a 5 T magnet in a range from 2 to 300 K. Samples were powdered, contained in a gel bucket, and fixed in a nonmagnetic sample holder. Each raw data file for the measured magnetic moment was corrected for the diamagnetic contribution from the sample holder and the gel bucket. The molar susceptibility was corrected for diamagnetic contributions using Pascal's constants and the increment method. 2,4,6-Tris(*N*-methylhydrazino)-1,3,5-triazine was synthesized in close analogy to a published procedure.[17]

2,4,6-Tris{[*N*-methyl-*N*′-(pyridine-2-yl)methylidene]hydrazino}-1,3,5-triazine (L): A stirring solution of 2,4,6-tris(*N*-methylhydrazino)-1,3,5-triazine (1.3 g, 6 mmol, 1 equiv.) and pyridine-2-carboxaldehyde (1.73 mL,18.0 mmol, 3 equiv.) in methanol was heated to

reflux for 12 h, causing a white precipitate to form. This was collected by filtration, washed with methanol, and dried in air; yield 2.70 g (94%). ^{1}H NMR (500 MHz, [D$_6$]DMSO): δ = 8.62 (s, 3 H), 8.13 (d, 3 H), 8.01 (d, 3 H),7.93 (m, 3 H), 7.4 (m, 3 H), 3.78 (s, 3 H) ppm. ^{13}C{^{1}H} NMR (125.75 MHz, [D$_6$]DMSO): δ = 165.2, 154.4, 149.3, 139.7, 136.7, 123.6, 119.2, 30.9 ppm. IR (KBr): $\tilde{\nu}$ = 1586 w, 1545 m, 1517 w, 1483 w, 1462 m, 1417 m, 1389 m, 1333 m, 1289 w, 1213 w, 1167 m, 1033 s, 987 w, 912 w, 774 w, 741 w, 625 w cm^{-1}. MS (EI): *m*/*z* (%) = 480 (100) [M]$^+$. $C_{24}H_{24}N_{12}$ (480.2): calcd. C 59.99, H 5.03, N 34.98; found C 58.92, H 5.44, N 35.05.

[Mn^{II}(L)(NO$_3$)(H$_2$O)]·(NO$_3$)·*x*CH$_3$OH (1): A solution of L (100 mg, 0.208 mmol) and Mn(NO$_3$)$_2$·4H$_2$O (52 mg, 0.208 mmol) in methanol (20 mL) was stirred for 1 h at room temperature. Light yellow crystals of **1** were obtained by slow evaporation of the resulting solution; yield 87 mg (62%). IR (KBr): $\tilde{\nu}$ = 3420 br, 1577 w, 1564 w, 1529 w, 1490 m, 1466 m, 1421 m, 1384 s (NO$_3^-$), 1356 w, 1278 w, 1170 w, 1033 m, 905 w, 801 w, 778 cm^{-1} w. MS (ESI, MeOH): *m*/*z* (%) = 597 (36), [LMn(NO$_3$)]$^+$. $C_{24}H_{26}MnN_{14}O_7$·0.5CH$_3$OH (693.5): calcd. C 42.43, H 4.07, N 28.28; found C 42.13, H 4.16, N 28.51.

[Mn$^{II}_2$(L)$_2$(N$_3$)(NO$_3$)(H$_2$O)](NO$_3$)$_2$·*x*H$_2$O (2): 2.3 equiv. of solid Mn(NO$_3$)$_2$·4H$_2$O (60 mg, 0.260 mmol) were added to 1 equiv. of L (50 mg, 0.104 mmol) in methanol (50 mL). The reaction mixture was stirred for 1 h at room temperature before 1 equiv. of solid sodium azide (7 mg, 0.104 mmol) was added. The light yellow solution became deep yellow within 5 min and was stirred for a further 2 h at room temperature. Plate-shaped yellow crystals of **2** were obtained by slow evaporation of the solution; yield 55 mg (41%). IR (KBr): $\tilde{\nu}$ = 3406 br, 2108 m (N$_3^-$), 2061 (N$_3^-$), 1576 w, 1562 w, 1528 w, 1489 m, 1463 m, 1421 m, 1385 m (NO$_3^-$), 1355 m, 1277 w, 1172 w, 1034 m, 905 w, 800 w, 778 w cm^{-1}. $C_{48}H_{48}Mn_2N_{30}O_{10}$·H$_2$O (1333.0): calcd. C 43.25, H 3.78, N 31.52; found C 43.17, H 4.04, N 32.29.

[Mn^{II}(L)(N$_3$)$_2$]·2CH$_3$OH (3): 1 equiv. of solid Mn(NO$_3$)$_2$·4H$_2$O (26 mg, 0.104 mmol) was added to 1 equiv. of L (50 mg, 0.104 mmol) in methanol (50 mL). The reaction mixture was stirred for 1 h at room temperature before 2 equiv. of solid sodium azide (14 mg, 0.208 mmol) were added. The light solution became deep yellow within 5 min and was stirred for a further 2 h at room temperature. Plate-shaped yellow crystals of **3** were obtained by slow evaporation of the solution; yield 55 mg (77%). IR (KBr): $\tilde{\nu}$ = 3425 br, 2037 s (N$_3^-$), 1576 w, 1561 w, 1526 w, 1492 m, 1466 m, 1424 m, 1398 m, 1359 m, 1345 w, 1277 w, 1168 m, 1037 m, 1005 w, 920 w, 906 w, 799 w, 782 w, 748 w, 694 w cm^{-1}. $C_{24}H_{24}MnN_{18}$·0.5CH$_3$OH (635.5): calcd. C 46.30, H 4.12, N 39.67; found C 46.15, H 3.95, N 41.14.

[Mn^{II}(L)(N$_3$)]$_n$(NO$_3$)$_n$·*n*CH$_3$OH (4): 1 equiv. of solid Mn(NO$_3$)$_2$·4H$_2$O (26 mg, 0.104 mmol) was added to a solution of 1 equiv. of L (50 mg, 0.104 mmol) in methanol (50 mL). The reaction mixture was stirred for 1 h at room temperature before 1 equiv. of solid sodium azide (7 mg, 0.107 mmol) was added. The light yellow solution became deep yellow within 5 min and was stirred for a further 2 h at room temperature. Light yellow crystals were obtained by slow evaporation of the solution; yield 57 mg (82%). IR (KBr): $\tilde{\nu}$ = 2054 s (N$_3^-$), 1574 w, 1562 w, 1526 w, 1491 m, 1467 m, 1422 m, 1384 s (NO$_3^-$), 1355 m, 1342 w, 1278 w, 1174 m, 1035 m, 990 w, 906 w, 799 w, 780 w, 637 w cm^{-1}. $C_{24}H_{24}MnN_{16}O_3$·0.5CH$_3$OH (655.5): calcd. C 44.89, H 4.00, N 34.19; found C 43.99, H 4.12, N 34.15.

[Mn^{II}L(dca)(H$_2$O)](NO$_3$)·*x*CH$_3$OH·*x*H$_2$O (5): 1 equiv. of solid Mn(NO$_3$)$_2$·4H$_2$O (26 mg, 0.104 mmol) was added to a solution of 1 equiv. of L (50 mg, 0.104 mmol) in methanol (50 mL). The reaction mixture was stirred for 1 h at room temperature before 1 equiv. of solid sodium dicyanamide (9 mg, 0.107 mmol) was added. The light yellow solution became deep yellow within 5 min and was stirred for a further 2 h at room temperature. Yellow crystals of **5**

Table 5. Crystal data and refinement details **1**–**5**.

	1	**2**	**3**	**4**	**5**
Empirical formula	$C_{24}H_{26}MnN_{14}O_7$	$C_{48}H_{48}Mn_2N_{30}O_{10}$	$C_{26}H_{32}MnN_{18}O_2$	$C_{25}H_{28}MnN_{16}O_4$	$C_{26}H_{26}MnN_{16}O_4$
Formula weight	677.53	1315.04	683.64	671.57	681.57
Crystal size [mm^3]	0.50×0.48×0.44	0.24×0.18×0.06	0.41×0.22×0.16	0.50×0.34×0.13	0.50×0.28×0.24
Crystal system	triclinic	triclinic	triclinic	triclinic	triclinic
Space group	$P\bar{1}$ (No. 2)	$P\bar{1}$ (No. 2)	$P\bar{1}$ (No. 2)	$P\bar{1}$ (No. 2)	$P\bar{1}$ (No. 2)
a [Å]	7.6447(6)	14.2328(12)	11.2636(5)	6.7116(4)	10.4827(4)
b [Å]	14.3390(10)	14.4951(10)	12.7851(6)	14.4431(10)	12.6223(4)
c [Å]	14.4515(10)	15.2225(11)	13.4006(6)	15.0108(10)	14.2137(5)
α [°]	84.139(6)	93.583(6)	115.026(3)	92.697(6)	77.851(3)
β [°]	86.797(6)	103.199(6)	108.553(4)	98.606(5)	72.139(3)
γ [°]	82.866(6)	95.415(6)	99.712(4)	92.980(5)	69.838(3)
V [Å^3]	1562.2(2)	3032.4(4)	1550.96(12)	1434.55(16)	1668.78(10)
Z	2	2	2	2	2
ρ [g/cm^3]	1.440	1.440	1.464	1.555	1.356
F(000)	698	1352	710	694	702
μ [mm^{-1}]	0.488	0.497	0.484	0.525	0.453
T_{min}/T_{max}	–	–	0.8059/0.9460	0.7314/0.9032	–
θ range [°]	1.42–26.79	1.77–27.06	1.85–26.97	1.37–26.78	1.52–26.73
hkl range	±9, –16–18, ±18	–18–14, ±18, ±19	–14–12, ±16, –16–17	–8–7, ±18, ±18	–13–12, ±15, ±17
Measured reflections	19573	25953	17581	16376	21976
Unique reflections [*R*int]	6626 [0.0327]	12993 [0.1641]	6728 [0.0657]	6091 [0.0499]	7065 [0.0485]
Observed refl. [$I > 2\sigma(I)$]	5443	7703	5794	4687	6338
Data/restraints/parameters	6626/26/417	12993/28/803	6728/3/423	6091/0/421	7065/2/433
Goodness-of-fit (F^2)	1.024	1.009	1.041	1.041	1.064
*R*1, *wR*2 [$I > 2\sigma(I)$]	0.0811, 0.2172	0.0922, 0.2264	0.0409, 0.1066	0.0531, 0.1391	0.0430, 0.1169
*R*1, *wR*2 (all data)	0.0916, 0.2251	0.1458, 0.2554	0.0487, 0.1108	0.0705, 0.1501	0.0466, 0.1187
Residual el. density [e/Å^3]	–1.031/1.184	–1.138/1.093	–0.724/0.640	–1.064/0.574	–0.662/0.682

were obtained by slow evaporation of the solution; yield 57 mg (82%). IR (KBr): $\tilde{\nu}$ = 3420 br, (OH), 2061 w (dca), 2215 w (dca), 2154 s (dca), 2133 s (dca), 1565 m, 1563 m, 1528 w, 1492 m, 1466 m, 1425 m, 1396 w, 1384 s (NO_3^-), 1356 m, 1280 w, 1171 m, 1041 m, 906 w, 775 w cm^{-1}. $C_{26}H_{26}MnN_{16}O_4 \cdot 1.5H_2O$ (708.6): calcd. C 44.07, H 4.13, N 31.63; found C 43.90, H 4.12, N 34.05.

X-ray Crystallography: Crystal data and details of the data collection are given in Table 5. X-ray data were collected with a STOE IPDS II diffractometer (graphite-monochromated Mo-K_α radiation, λ = 0.71073 Å) using ω scans at –140 °C. The structures were solved by direct methods and refined on F^2 using all reflections with SHELX-97.[34] Most non-hydrogen atoms were refined anisotropically. Most hydrogen atoms were placed in calculated positions and assigned to an isotropic displacement parameter of 0.08 $Å^2$. The positional and isotropic thermal parameters of the hydrogen atom bound to O1 in **3** were refined without any restraints or constraints. In **1** and **5** DFIX restraints (d_{O-H} = 0.82 Å) were applied and oxygen bound hydrogen atoms were refined with a fixed isotropic displacement parameter of 0.08 $Å^2$. Hydrogen atoms of the water molecule in **2** could not be located. Disordered nitrate ions in **1** [occupancy factors: 0.644(7)/0.356(7)] and **2** [occupancy factors: 0.545(9)/0.455(9) and 0.554(8)/0.446(8)] were refined with SADI (d_{N-O}, $d_{O\cdots O}$) and FLAT restraints and EADP constraints. In **3** one azide and one methanol solvent molecule are disordered over two positions [occupancy factors: 0.872(3)/0.128(3)]. SADI restraints (d_{N-N}, d_{C-O}) and EADP constraints were used to model the disorder. Atoms of the disordered parts were refined isotropically. No satisfactory model for the disorder could be found for the disordered solvent molecules (H_2O and/or methanol) in **1**, **2**, and **5**. For further refinement, the contribution of the missing molecules was subtracted from the reflection data by the SQUEEZE[35] routine of the PLATON[36] program. Face-indexed absorption corrections for **3** and **4** were performed numerically with the program X-RED.[37]

CCDC-795360 (for **1**), -795361 (for **2**), -795362 (for **3**), -795363 (for **4**), and -795364 (for **5**) contain the supplementary crystallographic data for this paper. These data can be obtained free of charge from The Cambridge Crystallographic Data Centre via www.ccdc.cam.ac.uk/data_request/cif.

Acknowledgments

Financial support by the Deutsche Forschungsgemeinschaft (DFG) (Priority Program 1137 "Molecular Magnetism") is gratefully acknowledged.

[1] a) W. L. Leong, J. J. Vittal, *Chem. Rev.* ASAP; b) J.-P. Costes, L. Vendiera, W. Wernsdorfer, *Dalton Trans.* **2010**, 4886–4892; c) L. Bogani, A. Vindigni, R. Sessolia, D. Gatteschi, *J. Mater. Chem.* **2008**, *18*, 4750–4758; d) H. Miyasaka, N. Motokawa, S. Matsunaga, M. Yamashita, K. Sugimoto, T. Mori, N. Toyota, K. R. Dunbar, *J. Am. Chem. Soc.* **2010**, *132*, 1532–1544; e) P. Mahata, S. Natarajan, P. Panissod, M. Drillon, *J. Am. Chem. Soc.* **2009**, *131*, 10140–10150.

[2] *Magneto-Structural Correlations in Exchange-Coupled Systems* (Eds.: R. D. Willet, D. Gatteschi, O. Kahn), NATO ASI Series, Reidel, Dordrecht, The Netherlands, **1985**.

[3] a) *Molecular-Based Magnetic Materials: Theory, Techniques and Applications* (Eds.: M. M. Turnbull, T. Sugimoto, L. K. Thompson), ACS Symposium Series, n. 644, ACS, Washington **1996**; b) A. Caneschi, D. Gatteschi, L. Pardi, R. Sessoli, *Clusters, Chains and Layered Molecules: the Chemist's Way to Magnetic Materials*, in: *Perspectives in Coordination Chemistry* (Ed.: A. F. Williams), VCH, Weinheim, Germany, **1992**.

[4] a) J. Ribas, A. Escuer, M. Monfort, R. Vicente, R. Cortés, L. Lezama, T. Rojo, *Coord. Chem. Rev.* **1999**, *193–195*, 1027–1068; b) F. Meyer, H. Kozlowski, in: *Comprehensive Coordination Chemistry II* (Eds.: J. A. McCleverty, T. J. Meyer), Pergamon, **2004**, vol. 6, pp. 247–554.

[5] a) Z.-H. Ni, H.-Z. Kou, L. Zheng, Y.-H. Zhao, L.-F. Zhang, R.-J. Wang, A.-L. Cui, O. Sato, *Inorg. Chem.* **2005**, *44*, 4728–4736; b) A. Escuer, R. Vicente, J. Ribas, X. Solans, *Inorg. Chem.* **1995**, *34*, 1793–1798; c) M. A. Halcrow, J. C. Huffman, G. Christou, *Angew. Chem. Int. Ed. Engl.* **1995**, *34*, 889–891; d) F. Meyer, S. Demeshko, G. Leibeling, B. Kersting, E. Kaifer, *Chem. Eur. J.* **2005**, *11*, 1518–1526; e) G. S. Papaefstathiou, S. P. Perlepes, A. Escuer, R. Vicente, M. Font-Bardia, X. Solans, *Angew. Chem. Int. Ed.* **2001**, *40*, 884–886; f) F. Meyer, P. Kircher, H. Pritzkow, *Chem. Commun.* **2003**, 774–775; g) S. Demeshko, G. Leibeling, W. Maringgele, F. Meyer, C. Mennerich, H.-H. Klauss, H. Pritzkow, *Inorg. Chem.* **2005**, *44*, 519–528; h) P. Mialane, A. Dolbecq, J. Marrot, E. Rivière, F. Sécheresse, *Chem. Eur. J.* **2005**, *11*, 1771–1778.

[6] a) Y.-Q. Wang, Q.-X. Jia, K. Wang, A.-L. Cheng, E.-Q. Gao, *Inorg. Chem.* **2010**, *49*, 1551–1560; b) X.-Y. Wang, Z.-M. Wang, S. Gao, *Chem. Commun.* **2008**, *3*, 281–294; c) Y.-F. Zeng, X. Hu, F.-C. Liu, X.-H. Bu, *Chem. Soc. Rev.* **2009**, *38*, 469–480; d) A. Escuer, G. Aromí, *Eur. J. Inorg. Chem.* **2006**, *23*, 4721–4736.

[7] a) S. Sasmal, S. Hazra, P. Kundu, S. Majumder, N. Aliaga-Alcalde, E. Ruiz, S. Mohanta, *Inorg. Chem.* **2010**, *49*, 9517–9526; b) P. Chaudhuri, R. Wagner, S. Khanra, T. Weyhermueller, *Dalton Trans.* **2006**, 4962–4968; c) S. Demeshko, G. Leibeling, S. Dechert, F. Meyer, *Dalton Trans.* **2006**, 3458–3465.

[8] a) T. K. Maji, W. Kaneko, M. Ohba, S. Kitagawa, *Chem. Commun.* **2005**, 4613–4615; b) A. Das, G. M. Rosair, M. S. E. Fallah, J. Ribas, S. Mitra, *Inorg. Chem.* **2006**, *45*, 3301–3306.

[9] a) E.-Q. Gao, P.-P. Liu, Y.-Q. Wang, Q. Yue, Q.-L. Wang, *Chem. Eur. J.* **2009**, *15*, 1217–1226; b) H.-L. Sun, S. Gao, B.-Q. Ma, G. Su, S.-R. Batten, *Cryst. Growth Des.* **2005**, *5*, 269–277; c) E.-Q. Gao, Z.-M. Wang, C.-H. Yan, *Chem. Commun.* **2003**, 1748–1749.

[10] a) C.-I. Yang, W. Wernsdorfer, G.-H. Lee, H.-L. Tsai, *J. Am. Chem. Soc.* **2007**, *129*, 456–457; b) T.-C. Stamatatos, K.-A. Abboud, W. Wernsdorfer, G. Christou, *Angew. Chem. Int. Ed.* **2007**, *46*, 844–888; c) A.-K. Boudalis, M. Pissas, C.-P. Raptopoulou, V. Psycharis, B. Abarca, R. Ballesteros, *Inorg. Chem.* **2008**, *47*, 10674–10681; d) T.-C. Stamatatos, K. A. Abboud, W. Wernsdorfer, G. Christou, *Angew. Chem. Int. Ed.* **2008**, *47*, 6694–6698.

[11] a) T. C. Stamatatos, K. A. Abboud, W. Wernsdorfer, G. Christou, *Inorg. Chem.* **2009**, *48*, 807–809; b) A. A. Massoud, M. A. M. Abu-Youssef, J. P. Vejpravova, V. Langera, L. Ohrstrom, *CrystEngComm* **2009**, *11*, 223–225.

[12] a) A. Escuer, R. Vicente, M. A. S. Goher, F. A. Mautner, *Inorg. Chem.* **1997**, *36*, 3440–3446; b) R. Cortes, M. Drillon, X. Solans, L. Lezama, T. Rojo, *Inorg. Chem.* **1997**, *36*, 677–683; c) E.-Q. Gao, Y.-F. Yue, S.-Q. Bai, Z. He, S.-W. Zhang, C.-H. Yan, *Chem. Mater.* **2004**, *16*, 1590–1596; d) M. A. M. Abu-Youssef, A. Escuer, M. A. S. Goher, F. A. Mautner, G. J. Reiß, R. Vicente, *Angew. Chem. Int. Ed.* **2000**, *39*, 1624–1626; e) L.-F. Tang, L. Zhang, L.-C. Li, P. Cheng, Z.-H. Wang, J.-T. Wang, *Inorg. Chem.* **1999**, *38*, 6326–6328.

[13] P. de Hoog, P. Gamez, L. W. Driessen, J. Reedijk, *Tetrahedron Lett.* **2002**, *43*, 6783–6786.

[14] a) P. Kopel, J. Mrozinski, K. Doležal, V. Langer, R. Boča, A. Biénko, A. Pochaba, *Eur. J. Inorg. Chem.* **2009**, 5475–5482; b) T. Glaser, T. Lügger, R. Fröhlich, *Eur. J. Inorg. Chem.* **2004**, 394–400; c) P. M. Lahti, Y. Liao, M. Julier, F. Palacio, *Synth. Met.* **2001**, *122*, 485–493.

[15] a) T. J. Mooibroek, P. Gamez, *Inorg. Chim. Acta* **2007**, *360*, 381–404; b) P. Gamez, J. Reedijk, *Eur. J. Inorg. Chem.* **2006**, 29–

42; c) A. Ranganathan, B. C. Heisen, I. Dix, F. Meyer, *Chem. Commun.* **2007**, 3637–3639.
[16] See, for example: a) V. A. Nikolakis, V. Exarchou, T. Jakusch, J. D. Woolins, A. M. Z. Slawin, T. Kiss, T. A. Kabano, *Dalton Trans.* **2010**, 9032–9038; b) Z. Lu, J. S. Costa, O. Roubeau, I. Mutikainen, U. Turpeinen, S. J. Teat, P. Gamez, J. Reedijk, *Dalton Trans.* **2008**, 3567–3573; c) I. Ekeltchik, J. Gun, O. Lev, R. Shelkov, A. Melman, *Dalton Trans.* **2006**, 1285–1293.
[17] For a structure proposal of 2,4,6-tris(methylhydrazino)-1,3,5-triazine, see: J. Wang, D. R. Miller, E. G. Gillan, *Carbon* **2003**, *41*, 2031–2037. The assumption is unlikely to be correct, since nucleophilic attack by NH_2NHMe occurs through the NHMe site rather than the NH_2 site; see also ref. [19].
[18] J. Ramirez, A.-M. Stadler, N. Kyritskas, J.-M. Lehn, *Chem. Commun.* **2007**, 237–239.
[19] J. Ramirez, A.-M. Stadler, L. Brelot, J.-M. Lehn, *Tetrahedron* **2008**, *64*, 8402–8410.
[20] a) G.-Y. Hsu, P. Misra, S.-C. Cheng, H.-H. Wei, S. Mohanta, *Polyhedron* **2006**, *25*, 3393–3398; b) M. Zhang, R. Fang, Q. Zhao, *J. Chem. Crystallogr.* **2008**, *38*, 601–604; c) P. Tyagi, U. P. Singh, *J. Coord. Chem.* **2009**, *62*, 1613–1622.
[21] a) S. T. Howard, *J. Am. Chem. Soc.* **1996**, *118*, 10269–10274; b) A. Göller, U.-W. Grummt, *Chem. Phys. Lett.* **2000**, *321*, 399–405.
[22] For selected examples, see: a) G. Marinescu, M. Andruh, M. Julve, F. Lloret, R. Llusar, S. Uriel, J. Vaissermann, *Cryst. Growth Des.* **2005**, *5*, 261–267; b) O. Jiménez-Sandoval, D. Ramírez-Rosales, M. d. J. Rosales-Hoz, M. E. Sosa-Torres, R. Zamorano-Ulloa, *J. Chem. Soc., Dalton Trans.* **1998**, 1551–1556; c) C. Paraschiv, J.-P. Sutter, M. Schmidtmann, A. Müller, M. Andruh, *Polyhedron* **2003**, *22*, 1611–1615; d) A. K. Sra, J.-P. Sutter, P. Guionneau, D. Chasseau, J. V. Yakhmi, O. Kahn, *Inorg. Chim. Acta* **2000**, *300–302*, 778–782.
[23] Simulation of the experimental magnetic data with a full-matrix diagonalisation of exchange coupling and Zeeman splitting was performed with the julX program (E. Bill, Max-Planck Institute for Bioinorganic Chemistry, Mülheim and der Ruhr, Germany).
[24] M. E. Fisher, *Am. J. Phys.* **1964**, *32*, 343–346.
[25] A. Escuer, R. Vicente, M. A. S. Goher, F. A. Mautner, *Inorg. Chem.* **1996**, *35*, 6386–6391.
[26] Z.-H. Ni, H.-Z. Kou, L. Zheng, Y.-H. Zhao, L.-F. Zhang, R.-J. Wang, A.-L. Cui, O. Sato, *Inorg. Chem.* **2005**, *44*, 4728–4736.
[27] A. K. Ghosh, D. Ghoshal, E. Zangrando, J. Ribas, N. Ray Chaudhuri, *Inorg. Chem.* **2005**, *44*, 1786–1793.
[28] T. K. Karmakar, G. Aromí, B. K. Ghosh, A. Usman, H.-K. Fun, T. Mallah, U. Behrens, X. Solans, S. K. Chandra, *J. Mater. Chem.* **2006**, *16*, 278–285.
[29] M. A. M. Abu-Youssef, A. Escuer, V. Langer, *Eur. J. Inorg. Chem.* **2005**, 4659–4664.
[30] H.-R. Wen, C.-F. Wang, Y. Song, J.-L. Zuo, X.-Z. You, *Inorg. Chem.* **2005**, *44*, 9039–9045.
[31] Z.-H. Zhang, X.-H. Bu, Z.-H. Ma, W.-M. Bu, Y. Tang, Q.-H. Zhao, *Polyhedron* **2000**, *19*, 1559–1566.
[32] X. Song, Y. Xu, L. Li, Z. Jiang, D. Liao, *Inorg. Chem. Commun.* **2006**, *9*, 1212–1214.
[33] H. G. O. Becker, W. Berger, G. Domschke, E. Fanghänel, J. Faust, M. Fischer, F. Gentz, K. Gewald, R. Gluch, R. Mayer, K. Müller, D. Pavel, H. Schmidt, K. Schollberg, K. Schwetlick, E. Seiler, G. Zeppenfeld, *Organikum*, 19th ed., J. A. Barth Verlag, Leipzig, Berlin, Heidelberg, **1993**, pp. 668.
[34] G. M. Sheldrick, *Acta Crystallogr., Sect. A* **2008**, *64*, 112–122.
[35] P. van der Sluis, A. L. Spek, *Acta Crystallogr., Sect. A* **1990**, *46*, 194–201.
[36] A. L. Spek, *Acta Crystallogr., Sect. A* **1990**, *46*, C34.
[37] STOE & CIE GmbH, *X-RED*, Darmstadt, Germany, **2002**.

Received: October 16, 2010
Published Online: January 27, 2011

